Structural Mechanics Based Model for the Force-Bearing Elements Within the Cytoskeleton of a Cell Adhered on a Bed of Posts

Amit Pathak
Department of Mechanical Engineering,
University of California,
Santa Barbara, CA 93106

Christopher S. Chen
Department of Bioengineering,
University of Pennsylvania,
Philadelphia, PA 19104

Anthony G. Evans
Department of Mechanical Engineering,
Materials Department,
University of California,
Santa Barbara, CA 93106

Robert M. McMeeking
Department of Mechanical Engineering,
Materials Department,
University of California,
Santa Barbara, CA 93106;
School of Engineering,
University of Aberdeen, King's College,
Aberdeen, AB24 3UE, Scotland;
INM—Leibniz Institute for New Materials,
Campus D2 2, 66123 Saarbrücken, Germany

*Mechanical forces play a vital role in the activities of cells and their interaction with biological and nonbiological material. Various experiments have successfully measured forces exerted by the cells when in contact with a substrate, but the intracellular contractile machinery leading to these actions is not entirely understood. Tan et al., (2003, "Cells Lying on a Bed of Microneedles: An Approach to Isolate Mechanical Force," Proc. Natl. Acad. Sci. USA, **100**(4), pp. 1484–1489) use a bed of PDMS posts as the substrate for cells and measure the localized mechanical forces exerted by the cell cytoskeleton on the posts. In live cell experiments for this setup, post deflections are measured, and from these results the forces applied by the cell are calculated. From such results, it is desirable to quantify the contractile tensions generated in the force-bearing elements corresponding to the stress fibers within the cell cytoskeleton that generate the loads applied to the posts. The purpose of the present article is to consider the cytoskeleton as a discrete network of force-bearing elements, and present a structural mechanics based methodology to estimate the configuration of the network, and the contractile tension in the corresponding stress fibers. The network of stress fibers is modeled as a structure of truss elements connected among the posts adhered to a single cell. In-plane force equilibrium among the network of stress fibers and the system of posts is utilized to calculate the tension forces in the network elements. A Moore-Penrose pseudo-inverse is used to solve the linear equations obtained from the mechanical equilibrium of the cell-posts system, thereby obtaining a least squares fit of the stress fiber tensions to the post deflections. The predicted network of force-bearing elements provides an approximated distribution of the prominent stress fibers connected among deflected posts, and the tensions in each fibril.* [DOI: 10.1115/1.4006452]

1 Introduction

Cells are small, deformable, highly sensitive structures, filled with an aqueous medium and enclosed in a flimsy plasma membrane; yet they are the very basis of all living organisms, including the strongest. The source of their capability is their ability to bond with the extra-cellular environment, and to support and generate substantial mechanical forces. Interaction of the cell with biological and nonbiological material involves mechanical forces, which are originated and supported by various structural elements of the cytoskeleton. Hence, the mechanical aspect of the structural organization of the cytoskeleton is of primary importance because various cell functions are directly related with cytoskeleton contractility, active remodeling, and deformability [1]. Cells react to external mechanical forces by altering the chemical activities that control the overall cytoskeletal organization and cell shape, regulated predominantly by actin filaments. The cytoskeleton structure is connected to the extra-cellular matrix or the cell substrate via integrin-ligand bond complexes, also known as focal adhesions, which act as anchors between the extra-cellular substrate and the cell, and are responsible for transmitting and supporting the mechanical forces generated by the cytoskeletal machinery. Actin filaments, in the form of stress fibers, are capable of generating intracellular mechanical forces, but little is known in a quantitative manner about this force generation, the formation of stress fibers, the variation of forces in the stress fibers, and the implication of these phenomena on overall cell behavior [2].

Various studies have shown that nanonewton-scale forces are exerted by the cell on its substrate; such forces are difficult to measure and analyze [3]. Several efforts have been made to track the deformations and traction forces generated by cells by mounting them on soft and compliant substrates [4–9]. For example, in some experiments, displacements of beads and microfabricated markers embedded in cells are analyzed in order to calculate the forces generated by them [4,10]. In such experiments, continuous or flat substrates allow extensive propagation of deformations, and the formation of many focal adhesions, making it hard to measure the deflection of the substrate at every single contact point [4,10,11]. Although these experiments provide important insights into the cell contractility, most of them have the limitation of being computationally intensive. On the other hand, experiments by Tan et al. [12] have had significant success in measuring the localized contractile forces generated by the cell when it comes in contact with a substrate. In these experiments, the cell is laid on a bed of microneedles (posts of PDMS), and makes focal adhesions only on top of the posts. This system results in a modest number of contact points, and deflection of the posts can be accurately measured and easily translated into a traction force map for the cell [12]. In this paper, we present a modeling methodology to quantify the forces in the intracellular actin network observed experimentally in the cell-on-posts setup utilized by Tan et al. [12].

Contributed by the Applied Mechanics Division of ASME for publication in the JOURNAL OF APPLIED MECHANICS. Manuscript received November 18, 2011; final manuscript received January 18, 2012; accepted manuscript posted online March 26, 2012; published online September 26, 2012. Assoc. Editor: Vikram Deshpande.

 Copyright © 2012 by ASME

Downloaded From: http://appliedmechanics.asmedigitalcollection.asme.org/ on 01/15/2014 Terms of Use: http://asme.org/terms

An understanding of the forces exerted by actin fibrils can be used to elucidate the governing rules for cell interaction with their external environment. Previous modeling attempts include the consideration of the cell as an elastic shell surrounding a viscoelastic core [13–15], and the cell as an isotropic elastic medium [16]. Continuum approaches are based on the fact that the internal cellular microstructure functions on a smaller scale compared to the size of the cell, and therefore the contractility in the cell can be considered to be continuous throughout its volume. On the other hand, several other models treat the cytoskeleton as a network of discrete structural elements. In one such approach, the cell is modeled as a tensegrity structure made of compressive and tensile structural elements [2,17–20]. In another approach, the cell is treated as an interlinked structure of passive elements [21], and in a third, as a discrete set of elastic filaments [22]. These discrete fiber models do not incorporate actin-myosin contractility per se into the structural elements of the cytoskeleton network, though some utilize stress fiber shrinkage to simulate cytoskeletal force generation. In this context, it is well established that the cell cytoskeleton is an interconnected structure made of three types of filaments (actin, microtubules, and intermediate filaments), and that actin-myosin interaction is the origin of the contractile's force that are transmitted to the cell substrate via focal adhesions [2].

We note that we have developed a coupled chemo-biomechanical model separately for cell contractility, the development and remodeling of the actin-myosin cytoskeleton [23,24], and the formation and development of focal adhesions [25]. This other model parallels and duplicates the outcomes of the present paper by use of a continuum description of the cytoskeleton, and by coupling mechanosensitivie features into the chemical kinetics of the formation, remodeling and dispersion of the actin-myosin cytoskeleton. We believe that the continuum model as described in the above three papers is perhaps more versatile, capable of greater accuracy, and brings more complete insights into the biochemomechanical phenomena taking place within the cell. However, the discrete, truss-element based model described in the present paper has attractive features, and in many ways is the obvious simulation methodology for an actin-myosin cytoskeleton composed of discrete fibrils. Therefore, we feel it is appropriate to explore such a model, and to place its advantages and limitations in the literature, so that others can judge whether it represents a tool that they wish to take advantage of for the purpose of modeling cell mechanics. In this regard, we note that the discrete, truss-element model is capable of a degree of accuracy in its ability to simulate the location of the most prominent stress fibers in the cytoskeleton, and, by implication, the tensions within such dominant fibrils. In this regard, the model is biologically relevant, and may be significant in connection with tools that are needed for association with therapies, diseases and conditions controlled by the contractile machinery of the cell, at least as far as in vitro studies are concerned that use cells adhered to a bed of posts. Certainly, more accurate models are feasible, and, as noted above, we have pursued such advances ourselves. However, the simplicity and ease of computation involved in the use of the discrete, truss-element model has a certain attraction and utility; as in all engineering, the accuracy of a model must be balanced against the cost and complexity of its use, and different objectives demand different levels of modeling accuracy. We believe this point of view is appropriate for the biomechanics of cells, and, in this spirit, put forward in this paper our discrete, truss-element model for the actin-myosin cytoskeleton and the associated tensions in its fibrils.

In the model developed for this study, we incorporate contractility into the structure of the stress fibers, and simulate the cell for known deformations of the post bed utilized by Tan et al. [12] for their experiments. Since, the stress fibers are known to generate and exert the majority of intracellular forces, we assume close synonymity between the stress fibers and the force-bearing elements inside the cell cytoskeleton modeled in this study. First, we present a method to depict the actin fibril structure as a simple network, composed of a finite number of stress fibers such that all the posts covered by a single cell are connected with each other, as depicted in Fig. 1 and calculate the equivalent tensions exerted by the fibrils. Post deflections measured in the experiments are used to determine this solution for the tensions in the stress fibers. In the following sections, a brief biological background and a structural mechanics based methodology for calculating the tensions in the stress fiber network, along with a set of sample calculations, is presented.

2 Defining a Structure of Stress Fibers Within a Single Cell Adhered on Top of Posts

The experimental setup of Tan et al. [12] is utilized for the measurements presented here, and adopted as the basis of our modeling. In these experiments, arrays of closely spaced vertical microneedles (posts) of PDMS were designed and utilized to encourage cells to attach and spread across multiple posts. Only the tops of the posts are coated with *fibronectin*, hence restricting the cell to form focal adhesions there only, and the contractile forces generated by the cell lead to loads being applied to the tips of the microneedles. As a result, the posts are vertical cantilevers, and bend as the cell probes the surface and applies forces. The deflection of each post occurs independently of its neighbors, and reports the distribution of traction forces under the spread cell, where such tractions lie in the plane orthogonal to the axis of the posts. Note that the components of the traction forces parallel to the axis of the posts are not measured in the experimental setup of Tan et al. [12]. The forces applied by the cell are determined from measurements of the post deflections, and the forces and deflections are related through

$$F = k\delta, \quad k = \frac{3\pi D^4 E}{64L^3} \tag{1}$$

where F is the magnitude of the applied force, k is the stiffness of the post, δ is the deflection of the top of the post, aligned with the direction of the applied force, D is the diameter of the circular cross-section of the post, E is Young's modulus for PDMS, and L is the height of the post. Hence, the post behavior is treated as that of a simple spring with spring constant k. The spring constant of the posts in the relevant experiments and thus utilized for the present analysis is $k = 32\,\mathrm{nN}/\mu\mathrm{m}$.

Contractility generated by the actin bundles, also known as stress fibers, plays a vital role in overall cell response. Wang and Suo [26] show images where the stress fibers can be seen traversing the cytoskeleton, which suggests that similar stress fibers can be implicated for the interconnections among the posts in our

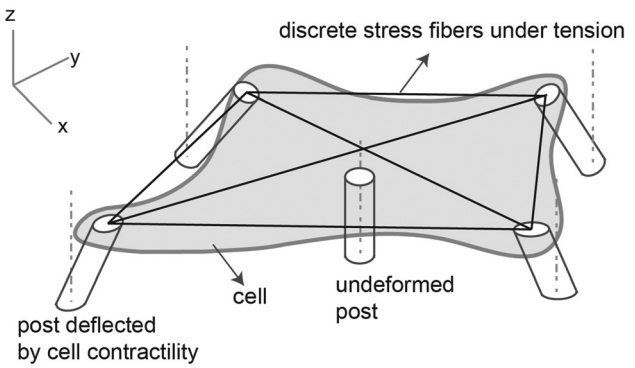

Fig. 1 A schematic depiction of a two-dimensional cell lying on top of a bed of posts, where the posts located near the periphery of the cell get deflected inward due to cell contractility. The cytoskeletal mesh responsible for cell contractility is proposed to be equivalent to a truss network composed tensile structural elements connected among the deflected posts.

Downloaded From: http://appliedmechanics.asmedigitalcollection.asme.org/ on 01/15/2014 Terms of Use: http://asme.org/terms

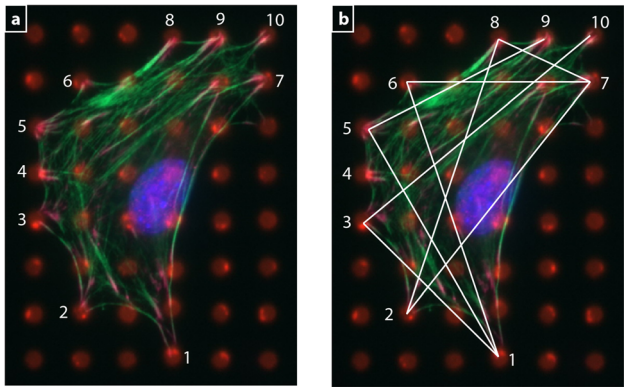

Fig. 2 (*a*) Top-view of the fibroblast cell adhered on a bed of PDMS posts, where the cytoskeleton is stained for F-actin. (*b*) Discrete truss elements are sketched arbitrarily by straight lines that represent the stress fibers equivalent to the overall actin mesh seen dispersed over the entire cell area. This network of truss elements is a pictorial representation of how an actual actin network can be replaced by finite number of discrete stress fibers that generates the equivalent effects of an actual cytoskeletal actin mesh. Here, 10 deflected posts at the periphery of the cell are marked.

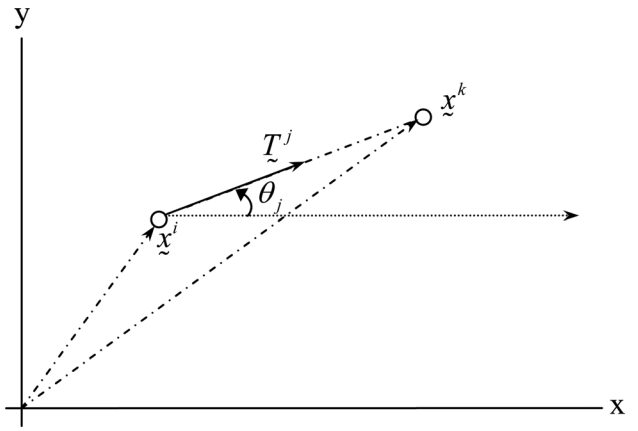

Fig. 3 Vector representation of a fibril originating from post *i* and terminating at post *k*, in a 2D Cartesian coordinate system. Here, x^i and x^k are the coordinates of the top of the posts, T^j is the tension in the fibril, oriented at an angle θ_j, connected between posts *i* and *k*.

setup. In other experiments, the cytoskeleton is stained for actin protein and the visual images suggest that stress fibers exist in the form of a mesh, as shown in Fig. 2(*a*) [2,23]. This actin mesh can be simplified in a somewhat arbitrary manner in terms of an equivalent, finite number of stress fibers that represent the actin mesh existent in the cell, as depicted in Fig. 2(*b*). This logic is used for depicting the actin mesh network as a structure of a finite number of equivalent stress fibers.

Consider the network of fibrils between all posts deflected by the cell at any moment; theoretically every post can be connected to every other post, *i.e.* the total number of possible connections among n_p posts is ${}^{n_p}C_2$, denoted as n_f. In-plane equilibrium of the contractile forces generated by the fibrils, and reaction forces associated with the deflected posts, provides governing equations for the system. In general, such a system will be statically indeterminate, since the number of independent equations provided by the condition of force equilibrium will be less than the number of unknown tensile forces in the fibrils. In order to solve the equations of such a structural system, we must reduce it to a tractable form while incorporating all possible interconnections among the posts. For such a structure, the total number of known parameters is $2n_p$, corresponding to the x and y components of the deflection of n_p posts, and the total number of unknown parameters is n_f, corresponding to the tension in each of the n_f fibrils.

In 2D space, the original, undisplaced position vectors of the tops of the posts, X, and the displacement vectors of the tops of the posts, u, are known. Thus, the deflected position vector of the i^{th} post can be obtained by using

$$\tilde{x}^i = \tilde{X}^i + \tilde{u}^i \tag{2}$$

where, $\tilde{X}^i$ is the position of the bottom of post i, $\tilde{u}^i$ is the displacement of the top of post i, and $\tilde{x}^i$ is the deflected position of the top of post i. For a network of fibrils connecting n_p posts, equilibrium for every post must be satisfied such that the contractile tension force in the fibrils causes the observed deflection of each post.

Assembly of the equilibrium equations is demonstrated as follows: a post i is connected with post k via a fibril j, as shown in Fig. 3, where $j = 1$ to n_f, given the total of n_f stress fibers in the system. Note that post i can only have $n_p - 1$ fibrils connecting it to the other $n_p - 1$ posts. Force equilibrium for post i can be stated as

$$\begin{aligned} ku_x^i &= \sum_{j=1}^{n_f} \cos\theta_j T_j \\ ku_y^i &= \sum_{j=1}^{n_f} \sin\theta_j T_j \end{aligned} \tag{3}$$

where k is the spring constant of the post, defined earlier in Eq. (1), θ_j is the positive angle formed by fibril j with the x-axis, and T_j is the tension in fibril j that connects post i to post k, as shown in Fig. 3. Compressive force in a fibril is allowed for, in which case T_j is negative; contractility of cable-like stress fibers rules out compressive force in it, but we must first compute the fibril tensions before we can identify any that are tending to have compressive forces generated within them. Note that, for purposes of consistency and completeness of fibril numbering, the summations in Eq. (3) include all stress fibers in the system whether they are connected to post i or not. If a given fibril is not connected to post i, the coefficient of T_j for that fibril is taken to be zero for the purposes of the summations in Eq. (3), so that the net force applied by fibrils to post i is correctly computed. Since there are n_p posts, and u_x^i and u_y^i are measured and thus known for each post, the results from Eq. (3), applied to every post in the system, give us $2n_p$ independent equations for the n_f unknown tensions in the fibrils. The $2n_p$ conditions from Eq. (3) are assembled as a set of linear equations written as

$$k\{u_p\} = [S]\{T_f\} \tag{4}$$

where $\{u_p\}^T = \left\{u_x^1 \;\; u_y^1 \;\; u_x^2 \;\; u_y^2 \ldots u_{n_p}^1 \;\; u_{n_p}^2\right\}$, $[S]$ contains the coefficients of T_j, consistent with Eq. (3), and $\{T_f\}^T = \{T_1 \;\; T_2 \ldots T_{n_f}\}$.

The coefficient matrix $[S]$, of size $2n_p \times n_f$, is not square other than for the case of 5 posts, since the number of fibrils is otherwise never equal to the number of posts divided by 2 when all posts are connected by fibrils to all other posts. Furthermore, force and moment equilibrium of the post bed by itself requires three of the post deflections to be dependent on the remainder, so that the maximum possible rank of $[S]$ is $r = 2n_p - 3$, or $r = n_f$, whichever is smaller. The rank, r, of the coefficient matrix $[S]$ in Eq. (4) dictates the number of independent equations, and an ideal system of equations that can yield a unique solution for $\{T_f\}$ corresponds to the case with $r = n_f$. This situation arises only for systems with either 2 or 3 posts, and all cases of $[S]$ with $n_p > 3$ are rank

Downloaded From: http://appliedmechanics.asmedigitalcollection.asme.org/ on 01/15/2014 Terms of Use: http://asme.org/terms

deficient, with $r < n_f$. To solve the resulting problem, we use the Moore-Penrose pseudo-inverse [27] to calculate the inverse of the coefficient matrix $[S]$. For rank deficient systems with $(r < n_f)$, this method calculates the minimum norm solution [27,28], *i.e.* it obtains the least square fit to Eq. (4) by minimizing

$$\varepsilon = \left([S]\{T_f\} - k\{u_p\}\right)^T \left([S]\{T_f\} - k\{u_p\}\right) \tag{5}$$

with respect to $\{T_f\}$. To do this, we employ the *pinv* function in MATLAB [29]. The function *pinv* uses a singular value decomposition method for factorization of the rectangular matrix to be inverted [28,29]. Tensions $\{T_f\}$ in the fibrils are then calculated using

$$\{T_f\} = k[S]^{\dagger}\{u_p\} \tag{6}$$

where $[S]^{\dagger}$ is the Moore-Penrose pseudo-inverse of the coefficient matrix $[S]$. The outcome of these calculations is that a definite set of fibril tensions is deduced. However, we cannot claim that the resulting set of tensions is unique, for we can always add a self equilibriated set of tensions to the result from Eq. (6), since such a set requires no force to be applied to the posts. The self-equilibriated set of tensions is that which can arise in a tensegrity structure [17,18], and lies in the null-space of $[S]$. However, the addition of such a self-equilibriated set means that the tension in some of the stress fibers will be reduced, and this reduction is logically restricted by the cable-like nature of stress fibers that requires us to avoid compression in them if feasible.

3 Sample Calculations

We utilize the same experimental setup reported in Tan et al. [12] with a square array of microposts with post radius $r = 1.5\,\mu$m, post bending stiffness $k = 32$ nN μm^{-1} and center-to-center post spacing $l = 10\,\mu$m. For a sample calculation, we use a dataset from these experiments, available as the top-view of posts deflected by an adhered single cell (Fig. 4). In these images, *white* circles represent the top-view of the undeflected posts, and deflected posts are seen as thick *whitish* lines. Within graphical accuracy, we obtain the post deflection data, u_x, and u_y, from the image and employ the procedure developed in the previous section to calculate the tension in stress fibers interconnected among the deflected posts.

We utilize the top-view (Fig. 4) with 6 deflected posts as an example to illustrate the procedure discussed earlier. Those posts having no visible deflection in Fig. 4 are omitted from the system. The measured deflections of the 6 active posts are listed in Table 1. Among 6 deflected posts a total of ${}^6C_2 = 15$ fibril interconnections are possible. Therefore, the rank of the resulting matrix $[S]$ is $2 \times 6 - 3 = 9$, substantially less than 15. We perform force calculations using Eqs. (3)–(6), where $n_p = 6$ and $n_f = 15$, and plot the results in Fig. 5. We find that the average tension in the stress fibers is 8.8 nN with a maximum of 20.6 nN. Exact tension values are listed in Table 2, where stress fibers are defined by their terminating post numbers, i and j. Note that the minimum tension value is negative, -1.5 nN, indicating compression. Such a result is unrealistic for a cable-like contractile stress fiber. In general, compressive forces in the cell cytoskeleton are supported by microtubules [11,30], which maintain force equilibrium with deflected posts and the contractile stress fiber network. Hence, we disqualify any truss elements under compression from the stress fiber network. Thus, we are able to model the actin mesh within the cytoskeleton for this particular example as a network of 14 equivalent stress fibers under positive tension connected among 6 deflected boundary posts and calculate the network specifications in terms of corresponding tensions, as plotted in Fig. 5.

In order to test the viability of this model in case of higher numbers of posts, we perform one additional calculation for the experimental data set in Fig. 2, where the contractile state of the cell is dictated by 10 deflected posts situated at the periphery of the cell. Here, ${}^{10}C_2 = 45$ fibrils will form a truss network connected among 10 deflected posts (deflections listed in Table 3). Similar to the

Table 1 List of x- and y-components of measured deflections of the 6 active posts marked in Fig. 5

	Measured post deflection (μm)	
Post number	x-component (u_x)	y-component (u_y)
1	−0.6	1.5
2	−0.6	0.6
3	−0.45	−0.6
4	0.6	0.45
5	1.2	−0.6
6	−0.9	−0.6

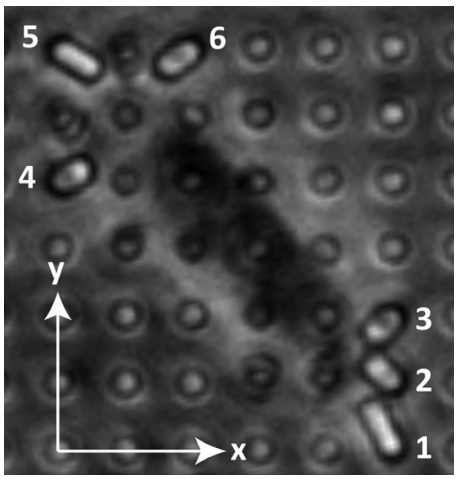

Fig. 4 A sample dataset for the top-view of the posts adhered to a single cell. Here, 6 posts deflected due to cell contractility are marked.

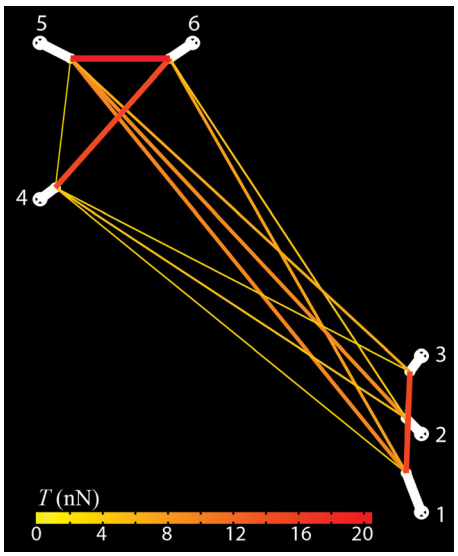

Fig. 5 Predicted structure of stress fibers on a 6 posts system corresponding to the experimental dataset (Fig. 4). Here, 14 equivalent fibrils represent the underlying actin mesh. Relative tensions in the stress fibers are illustrated according to the associated color map.

Downloaded From: http://appliedmechanics.asmedigitalcollection.asme.org/ on 01/15/2014 Terms of Use: http://asme.org/terms

Table 2 List of tensions in the network of stress fibers in Fig. 5, where individual fibrils are defined by the two connected posts *i* and *j*

Predicted tension in the fibril connecting posts *i* and *j* (nN)	*i*	*j*
8.4	1	2
18.2	1	3
3.3	1	4
11.6	1	5
8.8	1	6
9.6	2	3
5.2	2	4
11.2	2	5
5.1	2	6
3.9	3	4
7.5	3	5
2.5	4	5
17.8	4	6
20.6	5	6
−1.5	*3*	*6*

Table 3 List of x- and y-components of measured deflections of the 10 active posts marked in Fig. 2

	Measured post deflection (μm)	
Post number	x-component (u_x)	y-component (u_y)
1	−0.40	1.16
2	−0.09	0.54
3	0.54	−0.40
4	0.85	0.23
5	1.16	0.23
6	0.23	−0.09
7	−0.40	−0.40
8	−0.40	−1.02
9	−1.34	−1.02
10	−0.09	−0.71

previous calculation, we use Eqs. (3)–(6), with $n_p = 10$ and $n_f = 45$, to calculate forces in the fibrils, as listed in Table 4 and plotted in Fig. 6. We find that 12 out of 45 fibrils carry negative tensions, which must be disqualified from the stress fiber network. Note that the average tension in 33 stress fibers is 5.14 nN, which is significantly higher than the average compressive force, −1.66 nN, in the remaining 12 fibrils. Thus, we model a network of 33 stress fibers connected among 10 deflected posts and attribute the compressive forces to other structural components of the cell cytoskeleton such as microtubules. In the predicted network (Fig. 6), the general spatial distribution of the stress fibers matches well with the measured actin intensity in the experimental image in Fig. 2(*a*). Most notably, high tensions in the stress fibers around post numbers 5, 6, 8 and 9 in Fig. 6 corresponds with high intensity of stained actin in the same region of the cell in Fig. 2(*a*). In addition, these calculations also demonstrate that more than 90% of the total force exerted by the cytoskeletal fibrils lies in the tensile elements of the predicted network of discrete fibrils, which is in accord with the long-standing paradigm that suggests that the contractile state of the cell is mainly attributed to the tensile fibrils in the cell cytoskeleton. This qualitative agreement between model predictions and experimental measurements demonstrates that the presented force equilibrium based model can be used to predict the spatial distribution of prominent stress fibers, and that the results can be obtained through a relatively simple computation. Simultaneously, our model also highlights the basic limitations of any modeling framework that would use only the discrete elements to construct the cell cytoskeleton, and invokes the need, if higher levels of accuracy are desired, for more sophisticated

Table 4 List of tensions in the network of stress fibers in Fig. 6, where individual fibrils are defined by the two connected posts *i* and *j*

Predicted tension in the fibril connecting posts *i* & *j* (nN)	*i*	*j*
11.92	5	9
9.82	4	9
8.65	5	8
8.41	1	3
8.15	1	8
7.34	4	8
7.27	5	7
6.86	1	5
6.71	1	4
6.71	2	3
6.45	1	9
6.16	1	10
6.08	3	9
6.06	5	10
5.71	6	9
5.56	4	7
4.98	4	10
4.79	2	8
4.75	8	9
4.45	2	9
4.20	3	8
3.50	1	7
3.21	7	10
3.12	2	4
3.05	5	6
2.73	3	7
2.61	3	10
2.60	2	5
2.28	6	8
1.87	1	6
1.56	2	10
1.52	7	8
0.54	4	6
−0.09	*6*	*7*
−0.15	*2*	*7*
−0.24	*4*	*5*
−0.51	*1*	*2*
−0.62	*2*	*6*
−1.14	*6*	*10*
−2.34	*8*	*10*
−2.38	*3*	*4*
−3.02	*7*	*9*
−3.12	*3*	*5*
−3.15	*3*	*6*
−3.16	*9*	*10*

continuum models that can more readily capture the spatial resolution of the cytoskeleton distribution and the dynamic molecular mechanisms behind cell contractility.

4 Discussion

The overarching objective of this study is to develop a simple methodology for finding a network of equivalent stress fibers within a cell cytoskeleton for a cell-posts system. A definite fibril configuration along with associated tensile forces can be calculated for any cell adhered on top of a bed of posts using the Moore-Penrose pseudo-inverse method presented here. The evidence for the existence of cable-like actin bundles seen in experimental images, such as Fig. 2(*a*), inspired the approach of using discrete stress fibers in a cytoskeleton model, and we have successfully devised a scheme for modeling the contractility of the actin-myosin cytoskeleton in such a way. The methodology presented here provides an approach for identifying stress fibers equivalent to the mesh of actin-myosin bundles present in the cytoskeleton. These equivalent stress fibers are in the form of contractile truss elements, and become responsible

Downloaded From: http://appliedmechanics.asmedigitalcollection.asme.org/ on 01/15/2014 Terms of Use: http://asme.org/terms

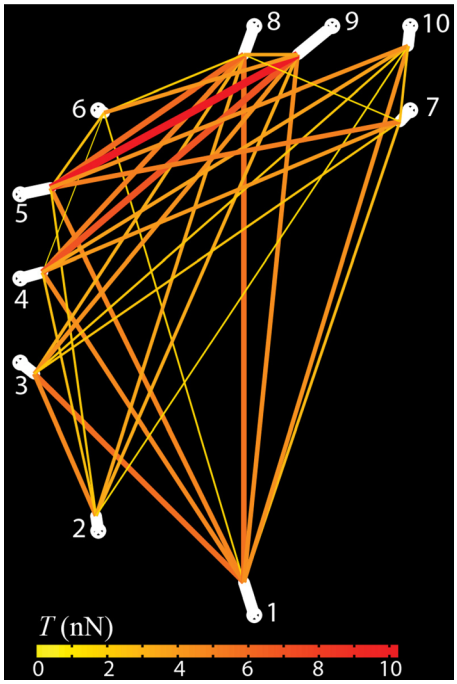

Fig. 6 Predicted network of stress fibers on a 10 posts system corresponding to the experimental dataset (Fig. 2(*a*)). Here, 33 equivalent fibrils represent the underlying actin mesh. Relative tensions in the stress fibers are illustrated according to the associated color map.

for the post deflections seen in the experiments. In addition, our method provides an estimate of the contractile tensions present in the individual equivalent stress fibers. Analytical and computational simplicity is an added feature of the model, especially in the case of complex cell-posts systems with a complicated actin meshwork and many equivalent stress fibers. An attractive feature of the technique presented in the current paper is that the analysis gives a definite result for the tensions in the equivalent stress fibers with little in the way of assumptions other than the idea that the Moore-Penrose pseudo-inverse is valid for solving the set of equations governing the structural mechanics of the system. The computations involved are relatively simple and easy to carry out, which we see as an advantage of the use of the discrete, truss-element based model that we have presented. Thus, the discrete representation of stress fibers in a structural mechanics based scheme as presented here is suitable for identifying the tensions in equivalent stress fibers at a given state of the system when the post deflections are in a measured configuration. Furthermore, the evolution of the tensions in the equivalent stress fibers can be traced by repeated analysis of the problem with updated post deflections representing the changing state of the system as the cell evolves its configuration in time. It would even be possible to add signaling and dynamic polymerization and depolymerization to the model to enable it to simulate the evolution of the stress fiber network, though some ingenuity would be required to accomplish such an objective. However, the development of such features is beyond the scope of the current work.

On the other hand, relevant limitations of the approach must be understood. One of the most significant drawbacks is that the result of the analysis is not unique. As we have noted above, in rank deficient systems we can always add a self-equilibriated set of stress fiber tensions to the results of the analysis and so the outcome is ambiguous, though constrained in this regard by the requirement that in cable-like networks, compressive truss loads should be avoided as much as possible. Furthermore, the methodology we have just presented and utilized is not a substitute for a fully characterized model of the actin-myosin cytoskeletal mechanics that includes appropriate constitutive laws for the behavior of the elements of the cell cytoskeleton. Such an approach was presented by Deshpande et al. [23–25]. Fully developed models of this type are capable of predicting important features of the cell behavior, such as cytoskeleton remodeling, actin polymerization/depolymerization, active contractility of the stress fibers in a manner dependent on the kinematics and biochemistry of the cell, and focal adhesion formation. In contrast, the approach utilized in the present paper so far simply provides a method for quantifying the tensions in a discrete set of equivalent stress fibers connecting posts to each other when the post deflections are known. While such results are potentially useful and give insights into the force levels generated internally within the actin-myosin stress fiber system, the method we have utilized in the present paper does not lend itself easily to extensions that would make it a predictive tool for the biochemomechanical constitutive behavior of the cytoskeleton, in that some ingenuity would be required to take such a step with the discrete model. Furthermore, it is not obvious how to generalize our method so that it may be applied to cells on flat substrates or embedded in the extracellular matrix, rather than adhered to posts. The system having posts provides a setup that enables a definite choice of a set of equivalent stress fibers joining each post to the others. When a cell is adhered to a flat surface, there is no obvious way to define a finite set of discrete equivalent stress fibers, other than in an arbitrary manner. The same point applies to a cell lying within an extracellular matrix, without discrete anchoring points for the cell, so that it is not obvious how to choose a finite set of discrete equivalent stress fibers to model the cytoskeleton for that case.

It can be argued that the techniques presented in the current paper can be augmented by visualization of the actin-myosin cytoskeleton, so that a set of tensions can be computed for an actual set of stress fibers instead of a hypothetical equivalent set of stress fibers. This concept is attractive because the consequent analysis would address the actual set of stress fibers that are causing the deflections of the posts rather than an arbitrary, assumed set. Furthermore, visualization of the stress fibers actually present in the cytoskeleton offers the possibility that the number to be analyzed will be less than ${}^{n_p}C_2$ due to some posts not being connected by stress fibers to all other posts. Therefore, the size of the matrix to be inverted by pseudo-inverse techniques may be reduced in size from the largest possibility, and thus the computational effort may be simpler than otherwise. Furthermore, it is even possible that the number of stress fibers to be analyzed is such that the rank of the resulting matrix is equal to the number of visualized fibrils. In that case, a set of equations will be established whose matrix of coefficients possesses a conventional, unique inverse, and the subsequent results for the tensions in the visualized stress fibers will be both unique and definite as the forces prevailing for that set of fibrils.

An example of a set of stress fibers visualized by actin staining is shown in Fig. 7 [24]. With such images, we have explored the problem of establishing the tensions in visualized stress fibers, given measured deflections of the posts [31]. However, the results have not been encouraging, and we have concluded that the methodology utilized is a *cul de sac*, and, given current visualization technology, cannot be built upon to improve our understanding of the mechanics of the actin-myosin cytoskeleton. In some cases, the results we have obtained from the approach described involves several fibrils subject to substantial compressive loads [31]. In other cases, we cannot find a subset of fibrils entirely in tension, where the ones tending to be in compression are omitted. Furthermore, the elimination of fibrils from the originally visualized set because they turn out to be in compression is counter to the idea that it is sufficient to visualize the stress fibers and to analyze the visualized set. In other cases, such as those depicted in Fig. 7, the visualized set of stress fibers presents a dilemma. It is apparent from the image in Fig. 7 that many of the post deflections, and thus the forces being applied by the stress fibers to the posts, are inclined obtusely to the axis of the visible fiber bundles. This situation implies that the tension in the stress fibers attached to the

Downloaded From: http://appliedmechanics.asmedigitalcollection.asme.org/ on 01/15/2014 Terms of Use: http://asme.org/terms

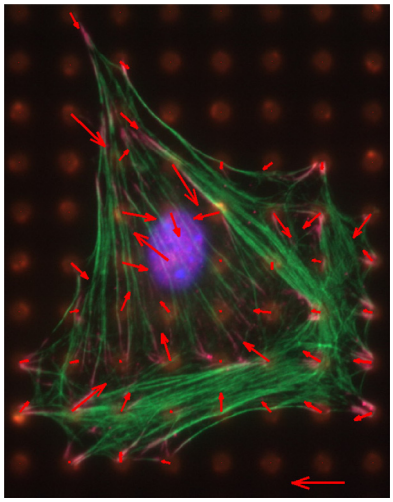

Fig. 7 Visualization is shown of a fibroblast cell on a bed of posts. The actin fibers are stained in green. The arrows represent force vectors, showing the deflection of the posts with the lengths of the arrows proportional to the force exerted by the cell on the posts [24].

relevant posts are extremely large, so that the projection of these tensions in the direction of the observed post deflection can be consistent with the magnitude of force being applied to the post (see Eq. (3)). Some post deflections are almost orthogonal to the visualized fibrils; a cable-like stress fiber that is orthogonal to the post deflection cannot be applying a force on that post in the direction of the post deflection. Thus, when the only visualized fibrils at a given post have an axis that is orthogonal to the observed post deflection, we have an inconsistency. Furthermore, in some cases, such as some in Fig. 7, the largest post deflections prevail for posts not having any visible stress fibers attached to them. Thus, if we assume that all actin is visualized by the staining procedure, and by the imaging of the cells, and we observe a deflection of a post that has no visualized actin attached to it, we have no way of rationalizing the observed post deflection. The implication of all these observations is that, in the case of some posts, the forces being applied to them are induced by actin-myosin that is not successfully visualized by the staining procedure. There are various possibilities why this may be so, including a failure to find the focal plane that will reveal a given stained fibril. Another possibility is that fine scale actin fibrils are not revealed by the relevant staining procedures, perhaps because the staining procedure is incapable of finding the very thin filaments, or cannot successfully attach the fluorescent dye to such fine actin fibrils. While the stress fibers network is a major component of the contractile apparatus of the cell cytoskeleton, the intracellular forces are also generated by several other important molecular mechanisms, such as polymerization of F-actin filaments at the leading edge that forms lamellipodial protrusions [32–34], and mechanosensitive adhesions that exist in transient and focalized states dispersed over the cell body [4,35,36]. Our conclusion is that often the visualized and recorded images of actin networks are not reliable, and therefore cannot be used as the basis of an analysis designed to identify the tension present in the set of active stress fibers that are causing the associated measured post deflections. As a consequence, the results of the mechanics analysis will be unreliable and will not provide any insights into the cytoskeletal mechanics prevailing. In such a situation, it seems better to assume that all posts are connected to all other posts by a stress fiber even if they are not visualized, and to carry out the analysis of the tension in the stress fibers through a Moore-Penrose pseudo-inverse, just as we have outlined the procedure in Sec. 2 above.

As noted above, we have found that a continuum model for the cell cytoskeleton, accounting for actin-myosin polymerization and depolymerization, fibril contractility, adhesion formation and associated mechanosensitive phenomena, is an attractive method for analyzing the mechanics of the cytoskeleton, because it is capable of predicting phenomena, such as how the cell distributes its actin-myosin fibrils, how it applied forces to posts, and how it generates focal complexes and focal adhesions [23–25]. The model is capable of simulating many observed phenomena in the behavior of cells in a mechanical setting [37,38]. For that work, we chose to use a continuum model where the stress fiber network is homogenized into a continuum field having attributes of actin-myosin concentration and the fibrillar orientation distribution. Such a continuum methodology is rather successful, even though stress fibers are often discrete and clearly visualized in images such as Fig. 6. We note, however, that the methodology adopted in [23–25] can be implemented, with some modifications and obvious restrictions, to a discrete set of stress fibers connecting each post to every other one. Thus, we observe that a predictive, constitutive based model can be implemented for a set of discrete fibrils. However, the discrete fibril concept seems to us to be most relevant to a cell attached to posts, and it is not so clear how one extends it to a cell on a flat substrate or to a cell embedded in extra-cellular matrix.

Nevertheless, the analytical technique we have presented in the current paper *is* a discrete stress fiber methodology, is relatively easy to use, can characterize the tensions in a discrete set of equivalent stress fibers for a cell on posts, and is capable of producing somewhat accurate, biologically relevant predictions of stress fiber networks and the associated tensions. As such, the effort to construct and utilize this method seems to us worthwhile.

Acknowledgment

This work was supported by the Army Research Office through the Multi University Research Initiative entitled "Bio-Mechanical Interfaces for Cell-Based Microsystems," Prime Award No. W911NF-04–1-071.

References

[1] Wang, N., Butler, J. P., and Ingber, D. E., 1993, "Mechanotransduction Across the Cell Surface and Through the Cytoskeleton," Science, **260**(5111), pp. 1124–1127.
[2] Alberts, B., Johnson, A., Lewis, J., Raff, M., Roberts, K., and Watson, J. D., 2002, *Molecular Biology of the Cell*, Garland Publishing, New York.
[3] Choquet, D., Felsenfeld, D. P., and Sheetz, M. P., 1997, "Extracellular Matrix Rigidity Causes Strengthening of Integrin-Cytoskeleton Linkages," Cell, **88**(1), pp. 39–48.
[4] Balaban, N. Q., Schwarz, U. S., Riveline, D., Goichberg, P., Tzur, G., Sabanay, I., Mahalu, D., Safran, S., Bershadsky, A., Addadi, L., and Geiger, B., 2001, "Force and Focal Adhesion Assembly: A Close Relationship Studied Using Elastic Micropatterned Substrates," Nat. Cell Biol., **3**(5), pp. 466–472.
[5] Burton, K., and Taylor, D. L., 1997, "Traction Forces of Cytokinesis Measured With Optically Modified Elastic Substrata," Nature, **385**(6615), pp. 450–454.
[6] Chrzanowska-Wodnicka, M., and Burridge, K., 1996, "Rho-Stimulated Contractility Drives the Formation of Stress Fibers and Focal Adhesions," J. Cell Biol., **133**(6), pp. 1403–1415.
[7] Harris, A. K., Wild, P., and Stopak, D., 1980, "Silicone Rubber Substrata: A New Wrinkle in the Study of Cell Locomotion," Science, **208**(4440), pp. 177–179.
[8] Pelham, R. J., and Wang, Y.-L., 1997, "Cell Locomotion and Focal Adhesions Are Regulated by Substrate Flexibility," Proc. Natl. Acad. Sci. USA, **94**(25), pp. 13661–13665.
[9] Riveline, D., Zamir, E., Balaban, N. Q., Schwarz, U. S., Ishizaki, T., Narumiya, S., Kam, Z., Geiger, B., and Bershadsky, A. D., 2001, "Focal Contacts as Mechanosensors: Externally Applied Local Mechanical Force Induces Growth of Focal Contacts by an Mdia1-Dependent and Rock-Independent Mechanism," J. Cell Biol., **153**(6), pp. 1175–1186.
[10] Dembo, M., Oliver, T., Ishihara, A., and Jacobson, K., 1996, "Imaging the Traction Stresses Exerted by Locomoting Cells With the Elastic Substratum Method," Biophys. J., **70**(4), pp. 2008–2022.
[11] Wang, N., Naruse, K., Stamenovic, D., Fredberg, J. J., Mijailovich, S. M., Tolic-Norrelykke, I. M., Polte, T., Mannix, R., and Ingber, D. E., 2001, "Mechanical Behavior in Living Cells Consistent With the Tensegrity Model," Proc. Natl. Acad. Sci. USA, **98**(14), pp. 7765–7770.
[12] Tan, J. L., Tien, J., Pirone, D. M., Gray, D. S., Bhadriraju, K., and Chen, C. S., 2003, "Cells Lying on a Bed of Microneedles: An Approach to Isolate Mechanical Force," Proc. Natl. Acad. Sci. USA, **100**(4), pp. 1484–1489.

Downloaded From: http://appliedmechanics.asmedigitalcollection.asme.org/ on 01/15/2014 Terms of Use: http://asme.org/terms

[13] Elson, E. L., 1988, "Cellular Mechanics as an Indicator of Cytoskeletal Structure and Function," Annu. Rev. Biophys. Bio., **17**(1), pp. 397–430.
[14] Evans, E., and Yeung, A., 1989, "Apparent Viscosity and Cortical Tension of Blood Granulocytes Determined by Micropipet Aspiration," Biophys. J., **56**(1), pp. 151–160.
[15] Fung, Y. C., and Liu, S. Q., 1993, "Elementary Mechanics of the Endothelium of Blood Vessels," J. Biomech. Eng., **115**(1), pp. 1–12.
[16] Nelson, C. M., Jean, R. P., Tan, J. L., Liu, W. F., Sniadecki, N. J., Spector, A. A., Chen, C. S., and Langer, R., 2005, "Emergent Patterns of Growth Controlled by Multicellular Form and Mechanics," Proc. Natl. Acad. Sci. USA, **102**(33), pp. 11594–11599.
[17] Ingber, D. E., 2003, "Tensegrity I. Cell Structure and Hierarchical Systems Biology," J. Cell Sci., **116**(7), pp. 1157–1173.
[18] Ingber, D. E., 2003, "Tensegrity II. How Structural Networks Influence Cellular Information Processing Networks," J. Cell Sci., **116**(8), pp. 1397–1408.
[19] Chen, C. S., Alonso, J. L., Ostuni, E., Whitesides, G. M., and Ingber, D. E., 2003, "Cell Shape Provides Global Control of Focal Adhesion Assembly," Biochem. Biophys. Res. Commun., **307**(2), pp. 355–361.
[20] Stamenovic, D., Fredberg, J. J., Wang, N., Butler, J. P., and Ingber, D. E., 1996, "A Microstructural Approach to Cytoskeletal Mechanics Based on Tensegrity," J. Theor. Biol., **181**(2), pp. 125–136.
[21] Satcher, R. L., Jr.,, and Dewey, C. F. Jr., 1996, "Theoretical Estimates of Mechanical Properties of the Endothelial Cell Cytoskeleton," Biophys. J., **71**(1), pp. 109–118.
[22] Mohrdieck, C., Wanner, A., Roos, W., Roth, A., Sackmann, E., Spatz, J. P., and Arzt, E., 2005, "A Theoretical Description of Elastic Pillar Substrates in Biophysical Experiments," ChemPhysChem, **6**(8), pp. 1492–1498.
[23] Deshpande, V. S., McMeeking, R. M., and Evans, A. G., 2007, "A Model for the Contractility of the Cytoskeleton Including the Effects of Stress-Fibre Formation and Dissociation," Proc. R. Soc. London, Ser. A-Math. Phy., **463**(2079), pp. 787–815.
[24] Deshpande, V. S., McMeeking, R. M., and Evans, A. G., 2006, "A Bio-Chemo-Mechanical Model for Cell Contractility," Proc. Natl. Acad. Sci. USA, **103**(38), pp. 14015–14020.
[25] Deshpande, V. S., Mrksich, M., McMeeking, R. M., and Evans, A. G., 2008, "A Bio-Mechanical Model for Coupling Cell Contractility With Focal Adhesion Formation," J. Mech. Phys. Solids, **56**(4), pp. 1484–1510.
[26] Wang, N., and Suo, Z., 2005, "Long-Distance Propagation of Forces in a Cell," Biochem. Biophys. Res. Commun., **328**(4), pp. 1133–1138.
[27] Meyer, C. D., 2001, *Matrix Analysis and Applied Linear Algebra*, SIAM: Society for Industrial and Applied Mathematics, Philadelphia, PA.
[28] Strang, G., 2003, *Introduction to Linear Algebra*, Wellesley-Cambridge Press, Wellesley, MA.
[29] MATLAB, 2007, *Reference Guide, V. R2007a*, The MathWorks, Inc., Natick, MA.
[30] Brangwynne, C. P., Mackintosh, F. C., Kumar, S., Geisse, N. A., Talbot, J., Mahadevan, L., Parker, K. K., Ingber, D. E., and Weitz, D. A., 2006, "Microtubules Can Bear Enhanced Compressive Loads in Living Cells Because of Lateral Reinforcement," J. Cell Biol., **173**(5), pp. 733–741.
[31] Pathak, A., 2009, "Computational Models for the Bio-Chemo-Mechanical Behavior of Cells in Diverse Extra-Cellular Settings," Ph.D. thesis, Department of Mechanical Engineering, University of California, Santa Barbara, CA.
[32] Hotulainen, P., and Lappalainen, P., 2006, "Stress Fibers Are Generated by Two Distinct Actin Assembly Mechanisms in Motile Cells," J. Cell Biol., **173**(3), pp. 383–394.
[33] Prass, M., Jacobson, K., Mogilner, A., and Radmacher, M., 2006, "Direct Measurement of the Lamellipodial Protrusive Force in a Migrating Cell," J. Cell Biol., **174**(6), pp. 767–772.
[34] Gardel, M. L., Shin, J. H., Mackintosh, F. C., Mahadevan, L., Matsudaira, P., and Weitz, D. A., 2004, "Elastic Behavior of Cross-Linked and Bundled Actin Networks," Science, **304**(5675), pp. 1301–1305.
[35] Burridge, K., and Chrzanowska-Wodnicka, M., 1996, "Focal Adhesions, Contractility, and Signaling," Ann. Rev. Cell Dev. Biol., **12**(1), pp. 463–519.
[36] Beningo, K. A., Dembo, M., Kaverina, I., Small, J. V., and Wang, Y.-L., 2001, "Nascent Focal Adhesions Are Responsible for the Generation of Strong Propulsive Forces in Migrating Fibroblasts," J. Cell Biol., **153**(4), pp. 881–888.
[37] Wei, Z., Deshpande, V. S., McMeeking, R. M., and Evans, A. G., 2008, "Analysis and Interpretation of Stress Fiber Organization in Cells Subject to Cyclic Stretch," J. Biomech. Eng., **130**(3), p. 031009.
[38] Pathak, A., Deshpande, V. S., McMeeking, R. M., and Evans, A. G., 2008, "The Simulation of Stress Fibre and Focal Adhesion Development in Cells on Patterned Substrates," J. R. Soc. Interface., **5**(22), pp. 507–524.

Downloaded From: http://appliedmechanics.asmedigitalcollection.asme.org/ on 01/15/2014 Terms of Use: http://asme.org/terms